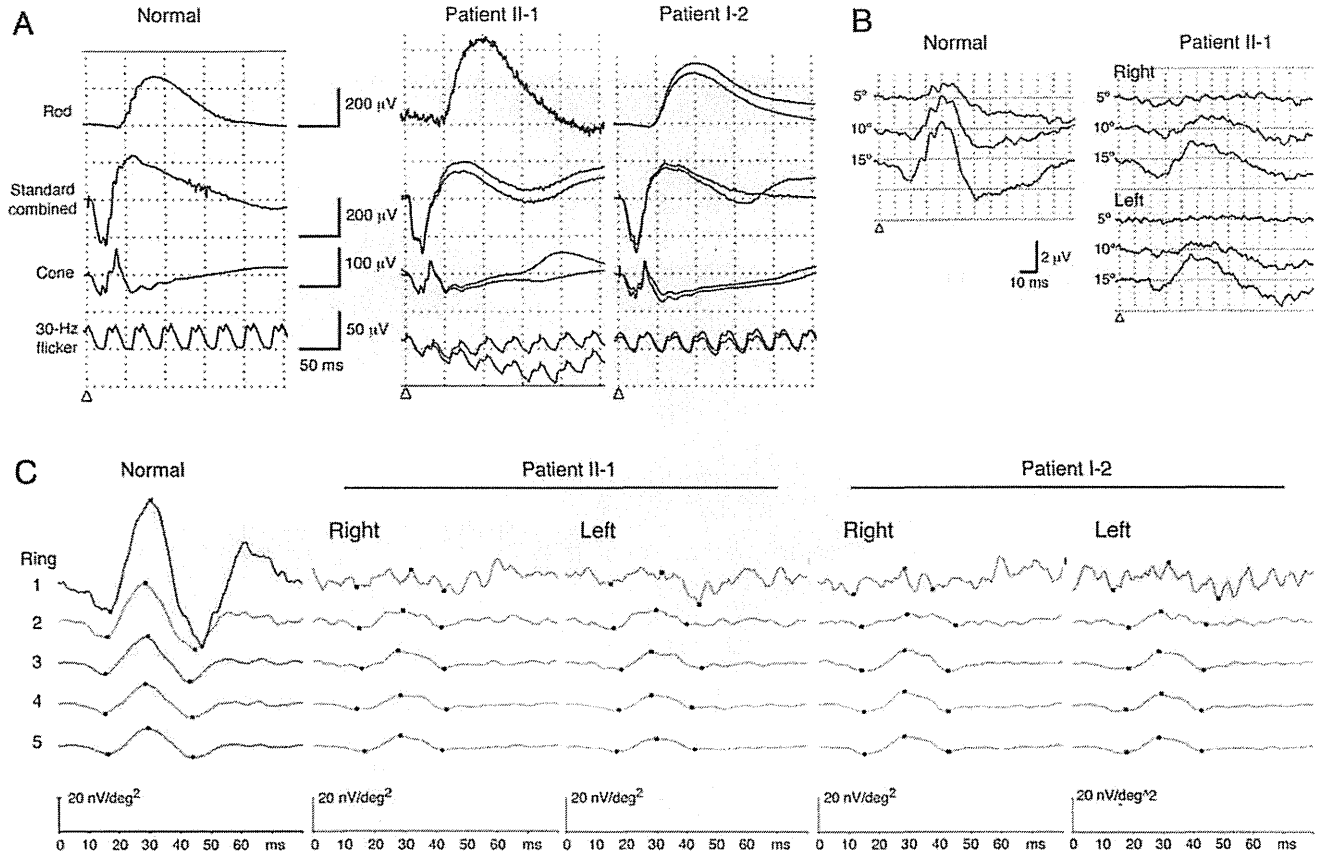

FIGURE 4.

Full-field ERG, focal macular ERG, and multifocal ERG. (A) Full-field ERG showed normal rod responses, normal standard combined responses, and slightly reduced photopic and 30-Hz flicker responses in patient II-1 at the age of 27 years and patient I-2 at the age of 70 years. (B) Focal macular ERG showed non-detectable responses at 5° spots, severely reduced responses at 10° spots, and reduced responses at 15° spots in patient II-1 at the age of 36 years. (C) Multifocal ERG showed absence of central (ring 1) responses, greatly reduced paracentral (ring 2) responses, and about one-third of normal responses in outer waveforms (rings 3 to 5) in patient II-1 at the age of 36 years and patient I-2 at the age of 70 years.

RP1L1 gene.[9] No other pathological variation of this gene was detected.

Although blood samples were available from the parents (I-1 and I-2) of patient II-1, none were obtained from the patient's mother's sister, who was also diagnosed with OMD. Like patient II-1, the affected mother (patient I-2) also carried a heterozygous mutation in the *RP1L1* gene, although the asymptomatic father (I-1) did not.

This mutation was not found in any of 100 Japanese individuals without any retinal diseases or in the Japanese single nucleotide polymorphisms database (http://snp.ims.u-tokyo.ac.jp).

DISCUSSION

At present, no studies have reported on the clinical features of OMD associated with *RP1L1* mutations since the discovery of those same mutations (p.R45W and p.W960R) in four Japanese families with autosomal dominant OMD.[9] In this study, both patients with the p.R45W mutation had ocular findings typical of OMD, markedly reduced central responses on either or both focal macular ERG (Fig. 4B) and multifocal ERG (Fig. 4C), and foveal structural abnormalities in the SD-OCT (Figs. 2C, 5C). However, ophthalmoscopic findings revealed subtle retinal pigment epithelium mottling (Fig. 5B) confirmed as small hyperfluorescent dots on FA in patient I-2 (Fig. 5A), although no similar abnormality was seen in patient II-1 (Fig. 2B). In addition to the ophthalmoscopic abnormalities in patient I-2, we observed slightly reduced photopic/30-Hz flicker responses (Fig. 4A) in both patients, findings which were unusual and differed from those previously reported,[1–3] as the diagnostic definition of OMD requires a normal ophthalmoscopic appearance and normal photopic/30-Hz flicker responses on full-field ERG. However, bull's eye maculopathy has been observed in only one patient of an autosomal dominant OMD family.[2]

Regarding OCT findings, a previous study first reported that mean foveal thickness in 11 patients with OMD was significantly thinner than in 20 age-matched controls[5]—a finding confirmed by subsequent reports[6,8,14]—demonstrating that foveal thickness determined using SD-OCT was thinned in all OMD patients. Foveal structural abnormalities observed using SD-OCT were recently reported in seven patients with autosomal dominant OMD, with IS/OS line irregularity at the foveal area noted in all seven, although *RP1L1* mutational analysis was not performed.[7] This previous observation of IS/OS line irregularity[7] was similar to the disorganized ELM and IS/OS lines noted in patient II-1 (Fig. 2C).

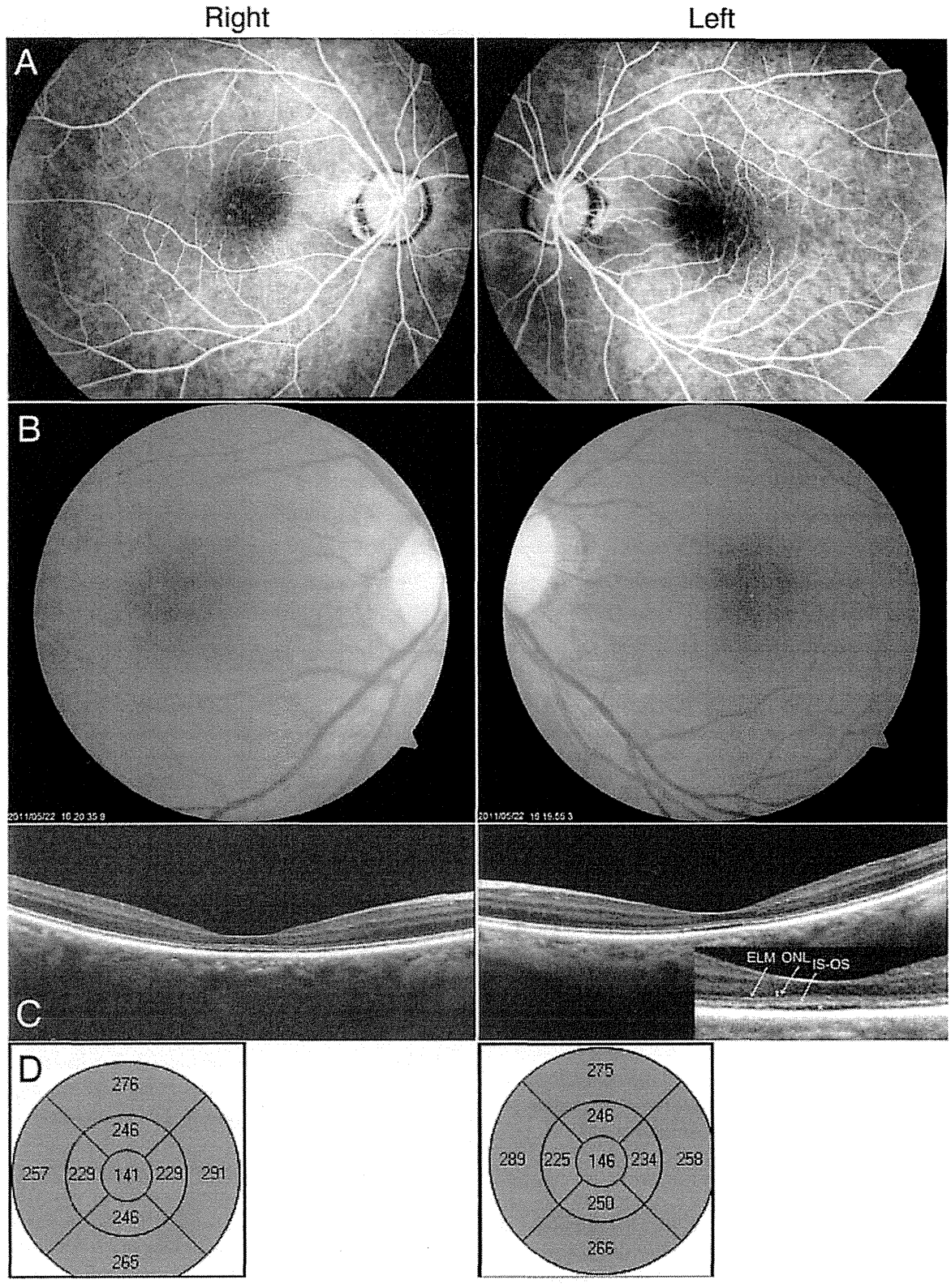

FIGURE 5.

Fluorescein angiograms, fundus photographs, and OCT findings in patient I-2. (A) Middle-phase fluorescein angiograms showed small hyperfluorescent dots due to retinal pigment epithelium alterations in the maculae at the age of 49 years. (B) Fundus photographs showed subtle retinal pigment epithelium mottling at the age of 70 years. (C) OCT images of the HD 5 line raster scan showed thinning of the ONL and discontinuous reflectivity of the ELM and IS/OS boundary at the foveal areas, and a hyporeflective zone (asterisk) can be seen between the IS/OS line and the hyperreflective retinal pigment epithelium/choriocapillaris band at the age of 70 years. (D) The macular thickness map of the Macular Cube protocol showed significant thinning within the 1- and 3-mm rings (red color) and normal thickness of the outer (3 to 6 mm) ring (green color).

In addition, macular thickness mapping revealed normal macular thickness (even in the central 1-mm ring) in patient II-1 (Fig. 2D) and significant thinning of the 1- and 3-mm rings associated with thinning of the ONL in patient I-2 (Fig. 5D). The normal macular thickness in patient II-1, who had relatively good visual fields (Fig. 3A), may be explained by the previous finding that some OMD patients do exhibit normal foveal thickness.[5,6]

A hyporeflective zone with either completely disrupted or discontinuous IS/OS junction reflectivity has been described in patients with achromatopsia[13] who have no functional cone photoreceptor cells. In this study, patient I-2 possessed such a hyporeflective zone with discontinuous reflectivity of the IS/OS lines at the foveal area (Fig. 5C), a phenomenon which has also been observed in other previously reported OMD patients.[8] Because cone photoreceptor density is maximal at the foveal region,[15,16] the hyporeflective zone present in patient I-2 resulted in a decreased number of cone photoreceptor cells, explaining the patient's color-vision and central visual-field defects (Fig. 3B), decreased visual acuity, and reduced multifocal ERG responses (Fig. 4C).

However, it should be noted that the above-mentioned SD-OCT findings differed between patients II-1 and I-2 with regard to foveal structure and ONL thickness. Differences in foveal structural abnormalities even between members of the same family may be due to differing levels of severity, differing disease stages, or phenotypic variability. Given that either preserved or thinned ONL thickness is relevant to disease progression, we hypothesize that foveal microstructural changes in the ELM and IS/OS lines with preserved foveal thickness are evident in early stages of the disease, as with patient II-1, whereas discontinuous reflectivity or disruption of the IS/OS lines with thinned foveal thickness are more typically observed in advanced stages, as with patient I-2. An SD-OCT study demonstrated that visual acuity was proportional to central foveal thickness in eight OMD patients,[6] supporting this hypothesis.

Despite the fact that the RP1L1 transcript and protein are expressed in both rod and cone photoreceptor cells,[12,17] all electroretinographic, visual-field, and SD-OCT abnormalities in these patients appear to be confined to the central retina. A recent study has suggested that both *RP1* and *RP1L1*, the genes of which share 63% identity at the amino acid level,[12,18] play essential and synergistic roles in photosensitivity and outer segment morphogenesis in photoreceptor cells.[19] *RP1* missense mutations and truncated mutations may be involved in the pathogenesis of autosomal dominant retinitis pigmentosa through a dominant negative effect.[20,21] Taken together, these findings suggest that the *RP1L1* mutation (p.R45W) may play a role in OMD etiology through a similar mechanism to *RP1* mutations, subsequently affecting the central retina with its maximum cone photoreceptor density.

In conclusion, this is the first report that described clinical characteristics of autosomal dominant OMD with the heterozygous mutation (p.R45W) in the *RP1L1* gene. Indeed, ophthalmoscopic macular changes and subtle reductions in photopic/30 Hz flicker responses can be seen in OMD patients with the mutation. SD-OCT findings differed between our patients and were indistinguishable from those obtained in other sporadic or *RP1L1*-unassociated OMD patients in whom other genetic loci may be involved. Further study will be required to determine whether *RP1L1* mutation-dependent clinical features are present.

ACKNOWLEDGMENTS

This work was supported by grants from the Ministry of Education, Culture, Sports, Science and Technology of Japan (Grant-in-Aid for Scientific Research; to TH); the Ministry of Health, Labor and Welfare of Japan (to TH); The Jikei University Research Fund (to TH); and the Vehicle Racing Commemorative Foundation (to TH and HT).

Received September 27, 2011; accepted November 4, 2011.

REFERENCES

1. Miyake Y, Ichikawa K, Shiose Y, Kawase Y. Hereditary macular dystrophy without visible fundus abnormality. Am J Ophthalmol 1989; 108:292–9.
2. Miyake Y, Horiguchi M, Tomita N, Kondo M, Tanikawa A, Takahashi H, Suzuki S, Terasaki H. Occult macular dystrophy. Am J Ophthalmol 1996;122:644–53.
3. Piao CH, Kondo M, Tanikawa A, Terasaki H, Miyake Y. Multifocal electroretinogram in occult macular dystrophy. Invest Ophthalmol Vis Sci 2000;41:513–7.
4. Lyons JS. Non-familial occult macular dystrophy. Doc Ophthalmol 2005;111:49–56.
5. Kondo M, Ito Y, Ueno S, Piao CH, Terasaki H, Miyake Y. Foveal thickness in occult macular dystrophy. Am J Ophthalmol 2003;135: 725–8.
6. Brockhurst RJ, Sandberg MA. Optical coherence tomography findings in occult macular dystrophy. Am J Ophthalmol 2007;143: 516–8.
7. Fujinami K, Tsunoda K, Hanazono G, Shinoda K, Ohde H, Miyake Y. Fundus autofluorescence in autosomal dominant occult macular dystrophy. Arch Ophthalmol 2011;129:597–602.
8. Kim YG, Baek SH, Moon SW, Lee HK, Kim US. Analysis of spectral domain optical coherence tomography findings in occult macular dystrophy. Acta Ophthalmol 2011;89:52–6.
9. Akahori M, Tsunoda K, Miyake Y, Fukuda Y, Ishiura H, Tsuji S, Usui T, Hatase T, Nakamura M, Ohde H, Itabashi T, Okamoto H, Takada Y, Iwata T. Dominant mutations in *RP1L1* are responsible for occult macular dystrophy. Am J Hum Genet 2010;87:424–9.
10. Hayashi T, Gekka T, Takeuchi T, Goto-Omoto S, Kitahara K. A novel homozygous *GRK1* mutation (P391H) in 2 siblings with Oguchi disease with markedly reduced cone responses. Ophthalmology 2007;114:134–41.
11. Takeuchi T, Hayashi T, Bedell M, Zhang K, Yamada H, Tsuneoka H. A novel haplotype with the R345W mutation in the *EFEMP1* gene associated with autosomal dominant drusen in a Japanese family. Invest Ophthalmol Vis Sci 2010;51:1643–50.
12. Bowne SJ, Daiger SP, Malone KA, Heckenlively JR, Kennan A, Humphries P, Hughbanks-Wheaton D, Birch DG, Liu Q, Pierce EA, Zuo J, Huang Q, Donovan DD, Sullivan LS. Characterization of *RP1L1*, a highly polymorphic paralog of the retinitis pigmentosa 1 (*RP1*) gene. Mol Vis 2003;9:129–37.
13. Thomas MG, Kumar A, Kohl S, Proudlock FA, Gottlob I. High-resolution in vivo imaging in achromatopsia. Ophthalmology 2011; 118:882–7.
14. Koizumi H, Maguire JI, Spaide RF. Spectral domain optical coherence tomographic findings of occult macular dystrophy. Ophthalmic Surg Lasers Imaging 2009;40:174–6.
15. Curcio CA, Sloan KR, Jr., Packer O, Hendrickson AE, Kalina RE. Distribution of cones in human and monkey retina: individual variability and radial asymmetry. Science 1987;236:579–82.

16. Chui TY, Song H, Burns SA. Adaptive-optics imaging of human cone photoreceptor distribution. J Opt Soc Am (A) 2008;25: 3021–9.
17. Conte I, Lestingi M, den Hollander A, Alfano G, Ziviello C, Pugliese M, Circolo D, Caccioppoli C, Ciccodicola A, Banfi S. Identification and characterisation of the retinitis pigmentosa 1-like1 gene (RP1L1): a novel candidate for retinal degenerations. Eur J Hum Genet 2003;11:155–62.
18. Blanton SH, Heckenlively JR, Cottingham AW, Friedman J, Sadler LA, Wagner M, Friedman LH, Daiger SP. Linkage mapping of autosomal dominant retinitis pigmentosa (RP1) to the pericentric region of human chromosome 8. Genomics 1991;11:857–69.
19. Yamashita T, Liu J, Gao J, LeNoue S, Wang C, Kaminoh J, Bowne SJ, Sullivan LS, Daiger SP, Zhang K, Fitzgerald ME, Kefalov VJ, Zuo J. Essential and synergistic roles of RP1 and RP1L1 in rod photoreceptor axoneme and retinitis pigmentosa. J Neurosci 2009;29: 9748–60.
20. Chiang SW, Wang DY, Chan WM, Tam PO, Chong KK, Lam DS, Pang CP. A novel missense RP1 mutation in retinitis pigmentosa. Eye (Lond) 2006;20:602–5.
21. Zhang X, Chen LJ, Law JP, Lai TY, Chiang SW, Tam PO, Chu KY, Wang N, Zhang M, Pang CP. Differential pattern of RP1 mutations in retinitis pigmentosa. Mol Vis 2010;16:1353–60.

Takaaki Hayashi
Department of Ophthalmology
The Jikei University School of Medicine
3-25-8 Nishi-shimbashi
Minato-ku, Tokyo 105-8461
Japan
e-mail: taka@jikei.ac.jp

Short Communication

Ophthalmic Research

Ophthalmic Res 2011;46:175–180
DOI: 10.1159/000325024

Received: October 22, 2010
Accepted after revision: February 3, 2011
Published online: March 29, 2011

Macular Dysfunction in Oguchi Disease with the Frequent Mutation 1147delA in the *SAG* Gene

Takaaki Hayashi[a] Satoshi Tsuzuranuki[a] Kenichi Kozaki[a] Mitsuyoshi Urashima[b] Hiroshi Tsuneoka[a]

[a]Department of Ophthalmology and [b]Division of Molecular Epidemiology, The Jikei University School of Medicine, Tokyo, Japan

Key Words
Full-field electroretinography · Multifocal electroretinography · Mutation · Optical coherence tomography · *SAG* gene

Abstract
Aim/Background: A 1-bp deletion (1147delA) in the *SAG* (also known as arrestin or S-antigen) gene is the most frequently seen mutation in Japanese patients suffering from Oguchi disease, a recessively inherited stationary night blindness. We investigated macular function in a patient with Oguchi disease with the 1147delA mutation. ***Methods:*** A 43-year-old Japanese male patient was diagnosed with Oguchi disease. The patient underwent complete ophthalmic examinations, including spectral-domain optical coherence tomography and Humphrey visual field testing. Full-field electroretinograms (ff-ERG) and multifocal ERG (mf-ERG) were recorded. Mutational analysis of the *SAG* gene was performed. ***Results:*** Corrected visual acuity was good in both eyes. Funduscopy showed retinal pigment epithelium atrophy along the vascular arcade bilaterally. The inner segment-outer segment (ISOS) boundary lines were preserved in the foveal and parafoveal areas, whereas ISOS boundary defects and thinning of the outer nuclear layer (ONL) were seen outside the preserved ISOS boundary. Humphrey testing showed significant paracentral field defects in both eyes. In addition to an absence of rod responses, cone and 30-Hz flicker responses were markedly reduced in ff-ERG. The central (ring 1) and paracentral (ring 2) responses with normal latencies were relatively preserved, but the outer waveforms (rings 3–5) were attenuated and prolonged in mf-ERG. The deletion mutation (1147delA) was identified homozygously. ***Conclusions:*** The reduced/delayed mf-ERG responses and visual field defects in paracentral macula areas are most likely to be correlated with ISOS boundary defects and thinning of the ONL. Macular dysfunction can occur in Oguchi disease with the 1147delA mutation in the *SAG* gene.

Introduction

Oguchi disease, first described in 1907 [1], is a rare autosomal-recessive form of congenital stationary night blindness, a non-progressive retinal disorder in which all other visual functions – including visual acuity, visual field, and color vision – are usually normal. One feature

KARGER

Fax +41 61 306 12 34
E-Mail karger@karger.ch
www.karger.com

0030–3747/11/0464–0175$38.00/0

Accessible online at:
www.karger.com/ore

Takaaki Hayashi, MD, PhD
Department of Ophthalmology, The Jikei University School of Medicine
3-25-8 Nishi-shimbashi, Minato-ku
Tokyo 105-8461 (Japan)
Tel. +81 3 3433 1111, ext. 3581, E-Mail taka@jikei.ac.jp

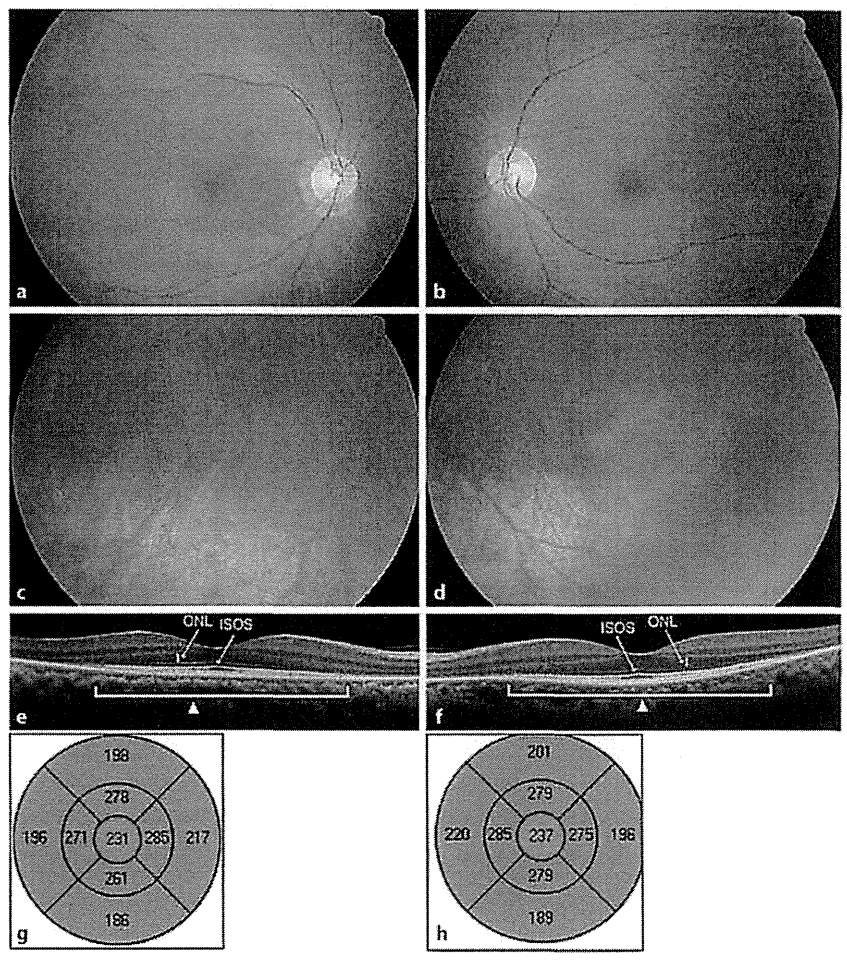

Fig. 1. Fundus photographs (**a–d**) and OCT findings (**e–h**). Retinal pigment epithelium atrophy is seen along the vascular arcade in OD (**a**) and OS (**b**). Golden-yellow discoloration is seen in the inferior mid-periphery in OD (**c**) and OS (**d**). ISOS boundary lines are preserved in the foveal and parafoveal areas (arrowheads), whereas ISOS boundary defects and thinning of the ONL are seen outside the preserved ISOS boundary in OD (**e**) and OS (**f**). The maps of macular thickness show preserved foveal thickness (green), but marked retinal thinning of the perifoveal region (red) in OD (**g**) and OS (**h**).

of the disease is a golden-yellow discoloration of the fundus that disappears in the long dark-adapted state (Mizuo-Nakamura phenomenon) [2]. Full-field electroretinograms (ff-ERG) show the absence of rod b-waves after 30 min of dark adaptation, and reduced a-waves and extremely reduced b-waves (negative type) in standard combined responses [3, 4]. In contrast, the single-flash cone and 30-Hz flicker responses are within normal limits [3, 4].

In 1995, a homozygous 1-bp deletion (1147delA, counted from the 5′ end of the previously published S-antigen cDNA sequence [5]) mutation in the *SAG* (also known as arrestin or S-antigen) gene was identified in 5 out of 6 unrelated Japanese patients with Oguchi disease [6]. Subsequently, 3 mutations [deletion of exon 5, Val380Asp, and Ser536 (4-bp del)] in the *GRK1* (rhodopsin kinase) gene were also reported in European patients with Oguchi disease [7]. The *SAG* mutation (1147delA), also called c.924delA (counted from the translation initiation site), has been most frequently seen in Japanese patients identified to date [8–12]. Saga et al. [11] demonstrated that a total of 9 Oguchi disease patients with the 1147delA mutation had the same haplotype at codon 403 and IVS6-18, suggesting that the 1147delA mutation may be inherited from a single founder. Although previous studies have shown the presence of reduced cone responses in some Oguchi disease patients with the frequent 1147delA mutation [8, 9], no studies have focused on the relationships between macular function and morphology.

This report was conducted to investigate macular function electroretinographically and anatomical features of the macula using optical coherence tomography (OCT) in an Oguchi disease patient with the frequent 1147delA mutation in the *SAG* gene.

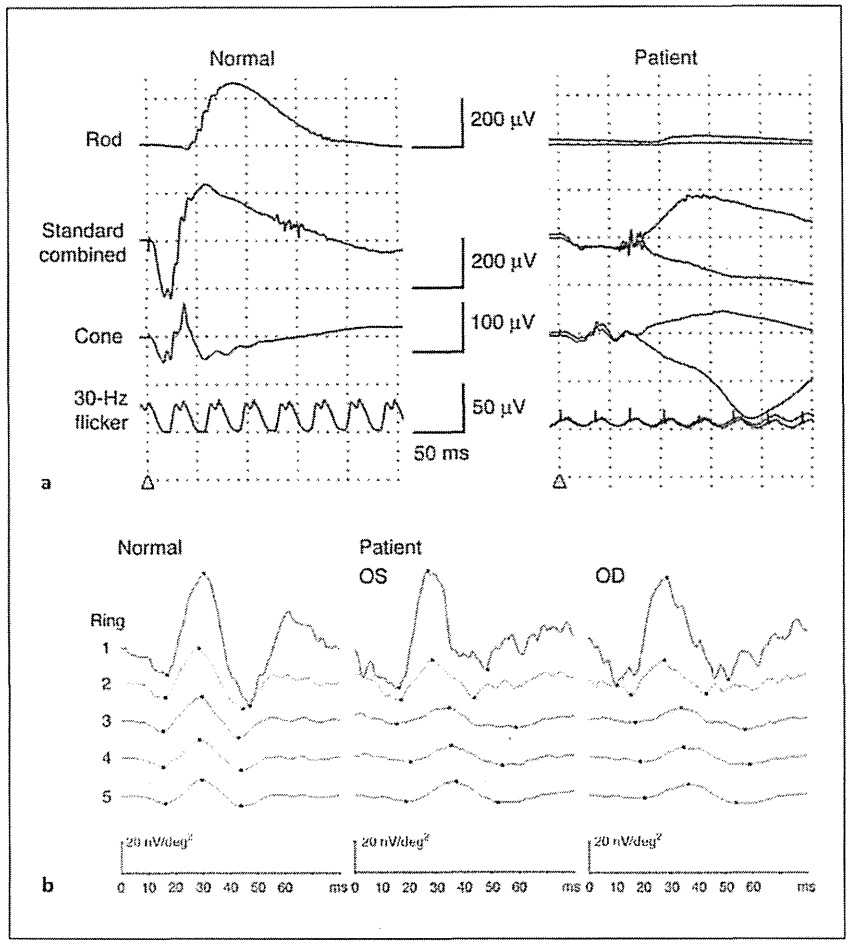

Fig. 2. ff-ERG (**a**) and mf-ERG (**b**). In the patient, ff-ERG (**a**) showed no rod responses, and an extreme reduction in a-wave amplitudes with almost extinguished b-wave amplitudes in standard combined ERG. Cone ERG revealed reduced responses in both a- and b-waves (approximately 25% of normal). Responses in 30-Hz flicker ERG showed reduced amplitudes (approximately 30% of normal). Ring averages (rings 1–5) of mf-ERG (**b**) are depicted. In the patient, the central (ring 1) and paracentral (ring 2) responses with normal latencies were relatively preserved, but the outer waveforms (rings 3–5) were attenuated and prolonged in both eyes.

Case Report

A 43-year-old Japanese male patient, who presented with a history of night blindness since childhood, was referred to our hospital. On the initial evaluation, his decimal best corrected visual acuity was 1.0 (sph –0.50, cyl –1.00, axis 35°) in oculus dexter (OD) and 1.5 (sph –0.25, cyl –0.75, axis 120°) in oculus sinister (OS). Anterior segments and media were unremarkable, except mild corneal opacity in both eyes. Funduscopy showed the retinal pigment epithelium atrophy along the vascular arcade (fig. 1a, b) and golden-yellow discoloration in the mid-periphery (fig. 1c, d), but there were neither retinal bone spicule pigmentation nor attenuation of the peripheral retinal vessels in both eyes. OCT (Cirrus HD-OCT, Carl Zeiss Meditec AG, Dublin, Calif., USA) showed that the inner segment-outer segment (ISOS) boundary lines were preserved in the foveal and parafoveal areas, consistent with the finding that best corrected visual acuity was normal; however, ISOS boundary defects and thinning of the outer nuclear layer (ONL) were seen outside the preserved ISOS boundary (fig. 1e, f). The maps of macular thickness demonstrated preserved foveal thickness, but marked retinal thinning of the perifoveal region in both eyes (fig. 1g, h).

The ff-ERG and multifocal ERG (mf-ERG) were recorded according to the International Society for Clinical Electrophysiology of Vision protocol, and the procedure and conditions have been reported previously [13, 14]. In the ff-ERG (fig. 2a), no rod responses were detected. Standard combined ERG showed an extreme reduction in a-wave amplitudes with almost extinguished b-wave amplitudes. Cone ERG results revealed reduced responses in both a- and b-waves (approximately 25% of normal in both eyes). Responses in 30-Hz flicker ERG showed reduced amplitudes (approximately 30% of normal in both eyes). Implicit times of all ff-ERG responses were normal. Ring averages (rings 1–5) of mf-ERG, recorded with a stimulus size of 61 hexagons, were measured. The central (ring 1) and paracentral (ring 2) responses with normal latencies were relatively preserved, but the outer waveforms (rings 3–5) were attenuated and prolonged in both eyes (fig. 2b).

For visual field assessment, the Humphrey Field Analyzer II (Carl Zeiss Meditec AG) was used to perform the central 30-2

Fig. 3. The pattern deviation plots using the Humphrey Field Analyzer II (**a**) show significant paracentral field defects in both eyes. Goldmann perimetry (**b**) shows no constriction of peripheral isopters (V-4e and I-4e), although the visual fields of the central isopter (I-2e) are moderately constricted in both eyes.

Swedish Interactive Threshold Algorithm standard program, showing significant paracentral field defects in the pattern deviation plots in both eyes (fig. 3a): the mean deviation was –3.55 dB ($p < 2\%$) in OS and –7.71 dB ($p < 0.5\%$) in OD; and the pattern standard deviation was 3.48 dB ($p < 2\%$) in OS and 3.69 dB ($p < 2\%$) in OD. On the other hand, Goldmann perimetry showed no constriction of peripheral isopters (V-4e and I-4e), although the visual fields of central isopter (I-2e) were moderately constricted in both eyes (fig. 3b), compatible with the Humphrey Field Analyzer findings.

For molecular genetic analysis, the research protocol was approved by the institutional review board of The Jikei University School of Medicine. The protocol adhered to the tenets of the Declaration of Helsinki, and informed consent was obtained from all participants. Coding regions of the *SAG* and the *GRK1* genes, containing exon/intron boundaries, were analyzed using polymerase chain reaction followed by sequencing as previously described [14]. A homozygous deletion mutation (1147delA or c.924delA) in exon 11 of the *SAG* gene was identified. No *GRK1* mutation was found in the patient. The patient's parents, who carry the 1147delA mutation heterozygously, had no ocular symptoms.

Discussion

Molecular genetic analysis identified a homozygous deletion mutation (1147delA) in the *SAG* gene, which is the most frequently seen mutation in Japanese patients with Oguchi disease identified to date [6, 8–12], although other *SAG* mutations (Arg175stop and Arg292stop) have also been identified [15]. Nakazawa et al. [8] reported 8 Oguchi disease patients with the 1147delA mutation, 3 of whom had slightly reduced 30-Hz flicker responses and constricted visual fields, similar to our patient's electroretinographic findings of markedly reduced cone and 30-Hz flicker responses (fig. 2a) and paracentral visual field defects (fig. 3a). Also, 1 of the 3 previously reported patients [8] and our patient had retinal pigment epithelium atrophy along the vascular arcade. These findings raise the possibility that cone dysfunction may be caused in some patients with 1147delA mutation-positive Oguchi disease.

The homozygous 1147delA mutation has been also found in 3 Japanese patients with retinitis pigmentosa, in whom pigmentary retinal degeneration and constriction of visual fields were identified [16]. Furthermore, Yoshii et al. [10] described 3 patients with the homozygous 1147delA mutation in a Japanese family, 2 of whom were diagnosed with Oguchi disease and 1 of whom (III-1, in the source publication) was diagnosed with retinitis pigmentosa. The patient (III-1) had a loss of visual acuity and severely constricted visual fields [10]. Our patient's findings of funduscopy (fig. 1) and Goldmann visual fields (fig. 3b) can be differentiated from those of retinitis pigmentosa. Taken together, the 1147delA mutation is likely to be associated with variable clinical expression, ranging from Oguchi disease with/without retinal pigment epithelium atrophy along the vascular arcade to retinitis pigmentosa. Azam et al. [17] reported 8 Oguchi disease patients in a Pakistani family, who had been given a diagnosis of autosomal recessive retinitis pigmentosa before a *GRK1* mutation (Ser205stop) was identified. Thus, genetic testing is important to confirm the definitive diagnosis of Oguchi disease because retinitis pigmentosa caused by the homozygous 1147delA mutation is an extremely rare form of retinal degenerative disorder.

Relationships between macular function and morphology have not been studied in Oguchi disease patients with the 1147delA mutation. When comparing cone-mediated mf-ERG (fig. 2b) with anatomical features of the macula (fig. 1e, f), the preserved central responses (rings 1 and 2) can be explained by the well-preserved ISOS boundary lines in foveal and parafoveal areas, whereas the attenuated outer waveforms (rings 3–5) are most likely caused by ISOS boundary defects and thinning of the ONL outside the preserved ISOS boundary. Recently, the outer retinal architecture has been investigated using spectral domain OCT in a patient with Oguchi disease before and after prolonged dark adaptation, demonstrating that the undetectable ISOS boundary line at the paramacular area was clearly detected after 4 h of dark adaptation, although mutation analysis was not performed [18]. The thickness of the ONL did not change between before and after prolonged dark adaptation [18], which seems to be inconsistent with our OCT findings. In fact, we tried to perform OCT after a prolonged dark adaptation. Regrettably, cooperation of the patient was not obtained. The OCT findings in our patient are also seen in patients with progressive retinal degenerative diseases such as retinitis pigmentosa [19]. Our findings indicate that macular dysfunction secondary to attenuated cone function can occur in Oguchi disease patients with the 1147delA mutation.

In conclusion, the reduced/delayed mf-ERG responses and visual field defects in paracentral macula areas most likely correlate with ISOS boundary defects and thinning of the ONL. Further study is needed to investigate whether macular dysfunction is seen in other Oguchi disease patients with the 1147delA mutation in the *SAG* gene.

Acknowledgements

This work was supported by grants from the Ministry of Education, Culture, Sports, Science and Technology of Japan (Grant-in-Aid for Scientific Research) (T.H.), The Jikei University Research Fund (T.H.), and the Vehicle Racing Commemorative Foundation (T.H. and H.T.).

Disclosure Statement

The authors have no proprietary or financial interest in any aspect of this study.

References

1 Oguchi C: Ueber eine Abart von Hemeralopie (in Japanese). Nippon Ganka Gakkai Zasshi 1907;11:123–134.
2 Mizuo G: A novel finding associated with function of dark adaptation in Oguchi disease (in Japanese). Nippon Ganka Gakkai Zasshi 1913;17:1148–1150.
3 Miyake Y, Horiguchi M, Suzuki S, Kondo M, Tanikawa A: Electrophysiological findings in patients with Oguchi's disease. Jpn J Ophthalmol 1996;40:511–519.
4 Hashimoto H, Kishi S: Shortening of the rod outer segment in Oguchi disease. Graefes Arch Clin Exp Ophthalmol 2009;247:1561–1563.
5 Yamaki K, Tsuda M, Shinohara T: The sequence of human retinal S-antigen reveals similarities with alpha-transducin. FEBS Lett 1988;234:39–43.
6 Fuchs S, Nakazawa M, Maw M, Tamai M, Oguchi Y, Gal A: A homozygous 1-base pair deletion in the arrestin gene is a frequent cause of Oguchi disease in Japanese. Nat Genet 1995;10:360–362.
7 Yamamoto S, Sippel KC, Berson EL, Dryja TP: Defects in the rhodopsin kinase gene in the Oguchi form of stationary night blindness. Nat Genet 1997;15:175–178.
8 Nakazawa M, Wada Y, Fuchs S, Gal A, Tamai M: Oguchi disease: phenotypic characteristics of patients with the frequent 1147delA mutation in the arrestin gene. Retina 1997;17:17–22.
9 Nakamachi Y, Nakamura M, Fujii S, Yamamoto M, Okubo K: Oguchi disease with sectoral retinitis pigmentosa harboring adenine deletion at position 1147 in the arrestin gene. Am J Ophthalmol 1998;125:249–251.
10 Yoshii M, Murakami A, Akeo K, Nakamura A, Shimoyama M, Ikeda Y, Kikuchi Y, Okisaka S, Yanashima K, Oguchi Y: Visual function and gene analysis in a family with Oguchi's disease. Ophthalmic Res 1998;30:394–401.
11 Saga M, Mashima Y, Kudoh J, Oguchi Y, Shimizu N: Gene analysis and evaluation of the single founder effect in Japanese patients with Oguchi disease. Jpn J Ophthalmol 2004;48:350–352.
12 Yoshida S, Yamaji Y, Yoshida A, Ikeda Y, Yamamoto K, Ishibashi T: Rapid detection of *SAG* 926delA mutation using real-time polymerase chain reaction. Mol Vis 2006;12:1552–1557.
13 Takeuchi T, Hayashi T, Bedell M, Zhang K, Yamada H, Tsuneoka H: A novel haplotype with the R345W mutation in the *EFEMP1* gene associated with autosomal dominant drusen in a Japanese family. Invest Ophthalmol Vis Sci 2010;51:1643–1650.
14 Hayashi T, Gekka T, Takeuchi T, Goto-Omoto S, Kitahara K: A novel homozygous *GRK1* mutation (P391H) in 2 siblings with Oguchi disease with markedly reduced cone responses. Ophthalmology 2007;114:134–141.
15 Nakamura M, Yamamoto S, Okada M, Ito S, Tano Y, Miyake Y: Novel mutations in the arrestin gene and associated clinical features in Japanese patients with Oguchi's disease. Ophthalmology 2004;111:1410–1414.
16 Nakazawa M, Wada Y, Tamai M: Arrestin gene mutations in autosomal recessive retinitis pigmentosa. Arch Ophthalmol 1998;116:498–501.
17 Azam M, Collin RW, Khan MI, Shah ST, Qureshi N, Ajmal M, den Hollander AI, Qamar R, Cremers FP: A novel mutation in *GRK1* causes Oguchi disease in a consanguineous Pakistani family. Mol Vis 2009;15:1788–1793.
18 Yamada K, Motomura Y, Matsumoto CS, Shinoda K, Nakatsuka K: Optical coherence tomographic evaluation of the outer retinal architecture in Oguchi disease. Jpn J Ophthalmol 2009;53:449–451.
19 Sugita T, Kondo M, Piao CH, Ito Y, Terasaki H: Correlation between macular volume and focal macular electroretinogram in patients with retinitis pigmentosa. Invest Ophthalmol Vis Sci 2008;49:3551–3558.

Eur J Ophthalmol 2011; 21 (5): 657-660 DOI: 10.5301/EJO.2011.6337

CASE REPORT

Improvement in S-cone–mediated visual fields and rod function after correction of vitamin A deficiency

Takaaki Hayashi, Tamaki Gekka, Tadashi Nakano, Hiroshi Tsuneoka

Department of Ophthalmology, The Jikei University School of Medicine, Tokyo - Japan

PURPOSE. *To evaluate S-cone–mediated visual fields and full-field electroretinograms (ERGs) in a patient with vitamin A deficiency.*

METHODS. *A 65-year-old woman diagnosed with primary sclerosing cholangitis reported experiencing night blindness. The patient underwent comprehensive ophthalmic examination, including funduscopy, ERGs, Humphrey standard automated perimetry (SAP), and short-wavelength automated perimetry (SWAP). Serum vitamin A concentrations were measured.*

RESULTS. *The patient's best-corrected visual acuity was 1.2 in both eyes. The ERG results showed no rod b-waves, reduced combined rod-plus-cone responses (negative type), and normal cone and 30-Hz flicker responses. Serum vitamin A concentration was 18 IU/dL (normal range 97-316 IU/dL). The SAP mean deviation (MD) values were –1.09 dB (OD) and –0.97 dB (OS), whereas the SWAP MD values were –10.10 dB (OD) and –10.50 dB (OS). The rate of sensitivity decreased with increasing eccentricity in SWAP. Four months after starting oral administration of vitamin A, all ERG values were normalized, and SWAP MD values were greatly improved (OD –3.47 dB, OS –4.10 dB) compared with changes in SAP MD values (OD +0.67 dB, OS +0.41 dB). Rod dysfunction and impaired S-cone–mediated pathways were preferentially observed and found to be reversed after the treatment.*

CONCLUSIONS. *The findings in this patient suggest that rods and S cones are more susceptible to vitamin A deficiency than L and M cones. Vitamin A deficiency visual impairment may therefore be reversible with appropriate therapy.*

KEY WORDS. *Full-field electroretinography, Short wavelength automated perimetry, Vitamin A deficiency*

Accepted: January 3, 2011

INTRODUCTION

Vitamin A is crucial for ocular metabolism. In the retinoid visual cycle (1), the retinal pigment epithelium traps all-*trans* retinol from choroidal circulation, at which point all-*trans* retinol is metabolized and converted to the crucial chromophore 11-*cis* retinal. This retinal is then transported to the rod outer segments, where it binds to rod opsins to generate rhodopsin.

The vitamin A derivative 11-*cis* retinal is also crucial to maintaining the function of cone opsins, including short wavelength-sensitive (S), middle wavelength-sensitive (M), and long wavelength-sensitive (L) cone opsins. These photoreceptor cells are also known to be involved in visual dysfunction occurring due to vitamin A deficiency (VAD), with the first sign of VAD usually cited as night blindness, followed by other visual disturbances. In developed countries, VAD is generally due to poor intestinal absorption, liver dysfunction, or bile duct obstruction (2).

Primary sclerosing cholangitis (PSC) is a chronic, progressive cholestatic disease characterized by diffuse inflammation and fibrosis of both intrahepatic and extrahepatic bile ducts. However, the etiology and pathogenesis of PSC are not yet well-understood. Here, we describe a PSC patient with VAD in whom static visual fields and full-field electroretinograms (ERGs) were evaluated before and 4 months after vitamin A treatment.

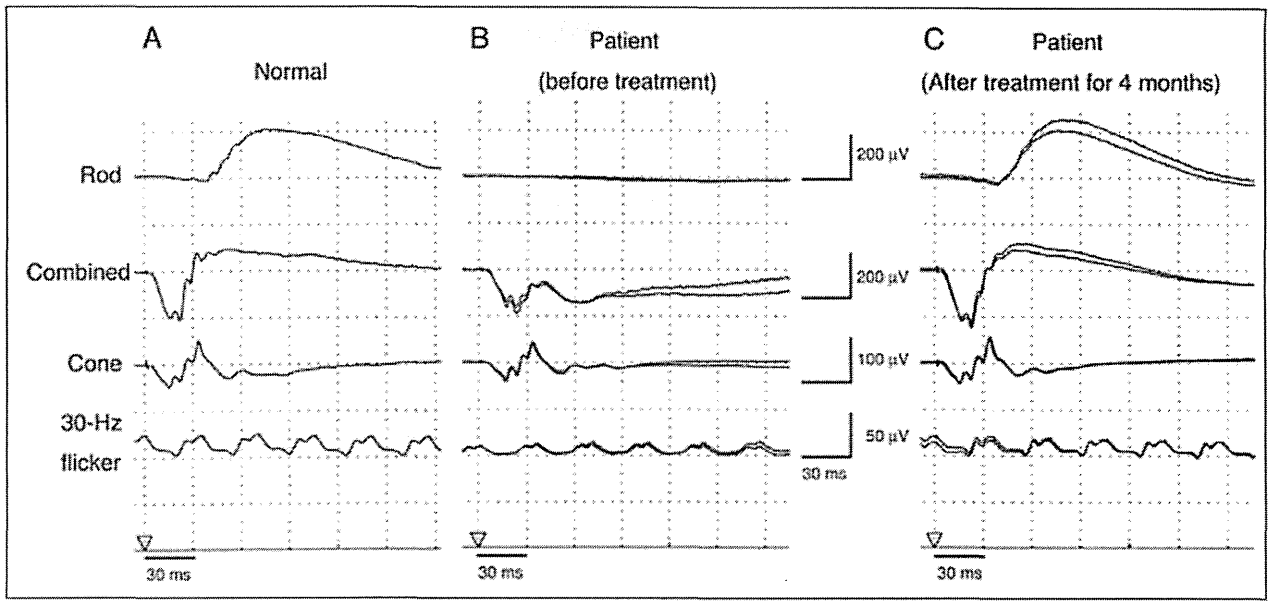

Fig. 1 - *Full-field electroretinograms (ERGs) from an age-matched normal subject with no retinal disease* **(A)** *and our vitamin A–deficient patient before* **(B)** *and 4 months after treatment* **(C)**. *Before treatment* **(B)**, *scotopic rod responses are undetectable, whereas photopic cone responses are well-preserved; however, the amplitudes of 30-Hz flicker ERGs are approximately half of normal* **(A)**. *Standard combined ERGs were negative-type with an additional a-wave amplitude reduction. Implicit times of all ERGs are nearly normal. After treatment* **(C)**, *all responses in rod, combined, cone, and 30-Hz flicker ERGs rebound to nearly normal levels.*

Case report

A 65-year-old Japanese woman was referred to our hospital following complaints of blurred vision and night blindness. She had been previously diagnosed with PSC, but had never had any ocular disease or received a blood transfusion. On initial evaluation at our hospital, the patient's best-corrected visual acuity was 1.2 in both eyes. No relative afferent pupillary defect was seen. Anterior segments and media were unremarkable except for the presence of mild senile cataracts in both eyes. Funduscopy showed no specific findings in either eye. Serum vitamin A concentration was markedly reduced at 18 IU/dL (normal range 97-316 IU/dL) (Tab. I). Electroretinogram were recorded according to the International Society for Clinical Electrophysiology of Vision protocol, as detailed previously (3). Scotopic rod responses were undetectable, whereas photopic cone responses were well-preserved; however, the amplitudes of 30-Hz flicker ERGs were approximately half of normal values (Fig. 1, A and B). Standard combined ERGs were negative-type with an additional a-wave amplitude reduction (Fig. 1B). Implicit times of rod, combined, cone, and 30-Hz flicker ERGs were nearly normal. Goldmann visual field testing was unremarkable.

We used the Humphrey Field Analyzer II (Carl Zeiss, Dublin, CA) to assess static visual fields, including central 30-2 Swedish interactive threshold algorithm (SITA), standard automated perimetry (SAP), and central 24-2 SITA short-wavelength automated perimetry (SWAP) programs. SWAP uses blue stimuli to stimulate S cones and a high-luminance yellow background to saturate L and M cones and rods (blue-on-yellow perimetry program). Mean deviation (MD), a global index that reflects overall depression in visual fields, was also evaluated. MD values for SITA-SAP were relatively well-preserved (–0.97 dB in OS, –1.09 dB in OD) (Fig. 2A). In contrast, SITA-SWAP results showed significant visual field loss, with MD values below –10 dB ($p<0.5\%$) in both eyes (Fig. 2C). The rate of sensitivity decreased with increasing eccentricity in SWAP (Fig. 2C). At this time, we confirmed that the impaired visual function was due to VAD secondary to PSC.

Treatment was initiated using oral administration of vitamin A (30,000 IU per day). At only 2 days after treatment, the serum vitamin A concentration had already increased to 95

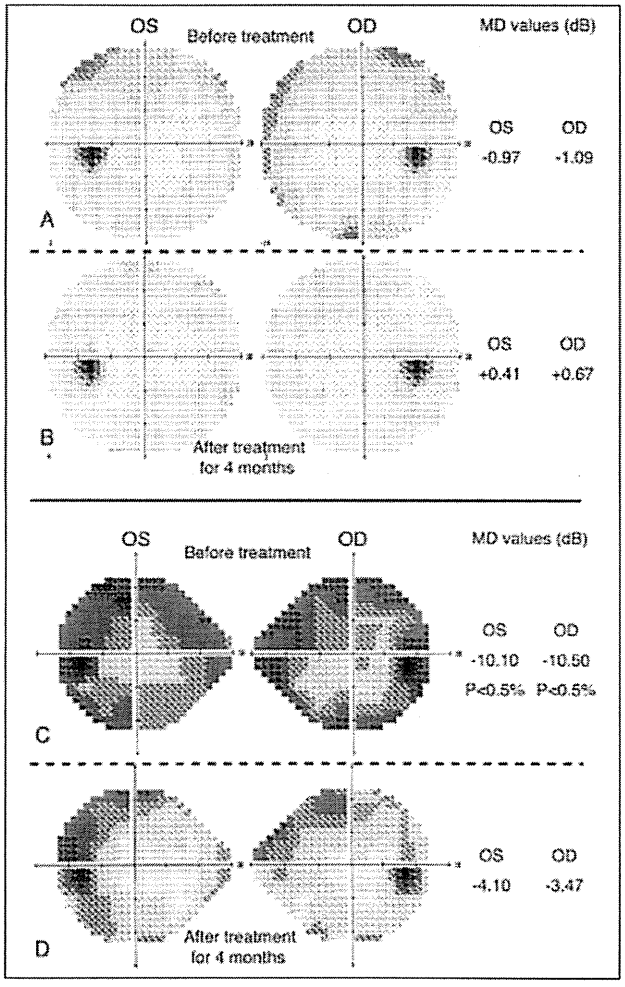

Fig. 2 - *Static visual fields using the Humphrey Field Analyzer II. Swedish interactive threshold algorithm (SITA)–standard automated perimetry (SAP) results before* **(A)** *and 4 months after treatment* **(B)**. *Swedish interactive threshold algorithm–standard automated perimetry results before* **(C)** *and 4 months after treatment* **(D)**. *See text for further details. Before treatment, MD values for SITA-SAP* **(A)** *are relatively well-preserved, whereas those for SITA-SWAP* **(C)** *are significantly low. After treatment, mean deviation (MD) values of SITA-SAP* **(B)** *remain unchanged or show subtle improvement, while SITA-SWAP* **(D)** *shows significant improvement in MD values.*

IU/dL (Tab. I), close to the normal range. The patient reported subjective improvements in night vision 4 to 8 weeks after treatment. Four months after the start of treatment, the ERG responses in rod, combined, cone, and 30-Hz flicker ERGs had rebounded to nearly normal levels (Fig. 1C). Mean deviation values of SITA-SAP remained unchanged or showed subtle improvement after treatment compared to before-treatment values (Fig. 2B), while SITA-SWAP showed significant improvement in MD values (–4.10 dB in OS and –3.47 in OD) (Fig. 2D). The patient continued to receive vitamin A treatment, and the concentration remained within the normal range for at least 7.5 months after treatment (Tab. I). The patient died of liver failure 16 months after initiation of vitamin A treatment.

DISCUSSION

With regard to ERG findings, before treatment, while the patient's rod responses were undetectable on ERG, the cone responses were relatively well-preserved (Fig. 1B), an observation consistent with the previous finding that rod dysfunction is typically observed earlier and is more extensive than cone dysfunction (2, 4). Although combined ERGs in most patients with VAD are subnormal, with reductions in both a-wave and b-wave amplitudes (4), the present patient showed negative ERG responses with reduced a-wave amplitudes, indicating not only the presence of photoreceptor abnormalities but also post-receptoral (or inner retinal transmission) dysfunction.

In their study, Newman et al (2) described 13 liver transplant candidates with VAD who were ophthalmologically asymptomatic, at least 5 of whom showed negative ERGs. The reason for the post-receptoral involvement remains unclear. Similar unexplained negative ERGs are also described in 34 cases of photoreceptor dystrophies reported by Koh et al (5), in keeping with previous reports on retinitis pigmentosa (RP), cone dystrophy, and cone-rod dystrophy (6). Additionally, Renner et al (7) described 47 patients with negative ERGs, 53% of whom had clinically suspected diagnoses (e.g., X-linked congenital retinoschisis, congenital stationary night blindness, and melanoma-associated reti-

TABLE I - SEQUENTIAL CHANGES IN SERUM VITAMIN A CONCENTRATION

Visit	Serum vitamin A concentration, IU/dL*
Before treatment	18
2 days after treatment	95
4 weeks after treatment	117
8 weeks after treatment	117
7.5 months after treatment	105

*Normal range: 97-316 IU/dL.

nopathy), whereas the remaining 47% showed unexpected post-receptoral dysfunction, such as cone (or cone-rod) dystrophy or RP. Thus, although the mechanism by which negative ERGs are induced remains unclear in VAD and hereditary photoreceptor disorders, post-receptoral dysfunction is strongly suspected to be a secondary effect.

With regard to cone dysfunction, considerable attention has been focused on which of the 3 cone classes is most susceptible to VAD. One report addresses this issue (4), finding that 2 of 3 patients with VAD had undetectable S-cone ERG responses, even though both these patients had borderline amplitude values in cone ERGs (4) with presumably preserved L- and M-cone function, findings which were similar to those in our present patient (Fig. 1B). To test the hypothesis that S-cone–mediated function is more severely affected than L- and M-cone–mediated function in VAD, we compared the results of SITA-SAP (Fig. 2A) with those of SITA-SWAP (Fig. 2C) in our patient. We noted that the MD values were much worse in SITA-SWAP than in SITA-SAP, suggesting that S-cone pathways were selectively affected before vitamin A treatment. Loss of the visual fields in SITA-SWAP was dramatically improved by vitamin A treatment (Fig. 2D). To our knowledge, this is the first report in which comparisons between white-on-white (SITA-SAP) and blue-on-yellow (SITA-SWAP) perimetries were performed before and after vitamin A treatment. Evaluation of both SITA-SAP and SITA-SWAP might be useful in clinical and diagnostic practice in patients with VAD. Taken together, our results support the hypothesis that S cones are indeed more vulnerable to VAD than L or M cones.

In conclusion, visual impairment due to VAD can be resolved with the application of appropriate therapy. Our findings suggest that rods and S cones are more susceptible to VAD than L or M cones. VAD should be considered as a potential cause of night blindness or unexplained visual loss, particularly in patients with clinically predisposing conditions, such as bile duct obstruction, malabsorption, or hepatic dysfunction.

Supported by grants from The Jikei University Research Fund (T.H.) and the Vehicle Racing Commemorative Foundation (T.H. and H.T.).

The authors report no proprietary interest.

Address for correspondence:
Takaaki Hayashi, MD, PhD
Department of Ophthalmology
The Jikei University School of Medicine
3-25-8 Nishi-shimbashi
Minato-ku, Tokyo, 105-8461, Japan
taka@jikei.ac.jp

REFERENCES

1. Saari JC. Biochemistry of visual pigment regeneration: the Friedenwald lecture. Invest Ophthalmol Vis Sci 2000; 41: 337-48.
2. Newman NJ, Capone A, Leeper HF, et al. Clinical and subclinical ophthalmic findings with retinol deficiency. Ophthalmology 1994; 101: 1077-83.
3. Hayashi T, Gekka T, Takeuchi T, Goto-Omoto S, Kitahara K. A novel homozygous *GRK1* mutation (P391H) in 2 siblings with Oguchi disease with markedly reduced cone responses. Ophthalmology 2007; 114: 134-41.
4. McBain VA, Egan CA, Pieris SJ, et al. Functional observations in vitamin A deficiency: diagnosis and time course of recovery. Eye 2007; 21: 367-76.
5. Koh AH, Hogg CR, Holder GE. The incidence of negative ERG in clinical practice. Doc Ophthalmol 2001; 102: 19-30.
6. Cideciyan AV, Jacobson SG. Negative electroretinograms in retinitis pigmentosa. Invest Ophthalmol Vis Sci 1993; 34: 3253-63.
7. Renner AB, Kellner U, Cropp E, Foerster MH. Dysfunction of transmission in the inner retina: incidence and clinical causes of negative electroretinogram. Graefes Arch Clin Exp Ophthalmol 2006; 244: 1467-73.

CLINICAL AND EXPERIMENTAL
OPTOMETRY

RESEARCH PAPER

Subfoveal choroidal thickness in multiple evanescent white dot syndrome

Clin Exp Optom 2012; 95: 212–217 DOI:10.1111/j.1444-0938.2011.00668.x

Ranko Aoyagi* MD
Takaaki Hayashi* MD PhD
Akiko Masai[†] MD
Katsuya Mitooka[†] MD PhD
Tamaki Gekka[§] MD PhD
Kenichi Kozaki* MD PhD
Hiroshi Tsuneoka* MD PhD
* Department of Ophthalmology, The Jikei University School of Medicine, Tokyo, Japan
[†] Department of Ophthalmology, Daisan Hospital, The Jikei University School of Medicine, Tokyo, Japan
[§] Department of Ophthalmology, Kashiwa Hospital, The Jikei University School of Medicine, Chiba, Japan
E-mail: taka@jikei.ac.jp

Submitted: 23 April 2011
Revised: 17 June 2011
Accepted for publication: 28 July 2011

Background: Multiple evanescent white dot syndrome (MEWDS) is an inflammation of the choriocapillaris, which typically presents with unilateral vision loss and is characterised by the presence of multiple yellow-white spots in the posterior pole to the midperipheral fundus. This study was conduced to evaluate subfoveal choroidal thickness between the acute and convalescent phases in two patients with MEWDS.

Methods: Two young female Japanese patients underwent a comprehensive ophthalmic examination, including slitlamp biomicroscopy, funduscopy and both fluorescein and indocyanine green angiographies. The subfoveal choroidal and central retinal thicknesses were measured using Cirrus high-definition spectral-domain optical coherence tomography.

Results: The two patients were diagnosed with unilateral MEWDS based on characteristic funduscopic and angiographic findings. The disrupted foveal inner segment–outer segment boundary line in the acute phase was restored in the convalescent phase in both patients. In the affected eye of Patient 1, the subfoveal choroidal thickness (337 μm) noted in the acute phase decreased to 249 μm at 133 days after the initial visit (convalescent phase). Similarly, the acute phase thickness (440 μm) in Patient 2 decreased to 358 μm at 133 days after the initial visit. The thickness in the asymptomatic opposite eye also decreased during the convalescent phase in both patients. In the acute phase, thickness in the affected eyes was greater than that in the opposite eyes in both patients. In contrast, central retinal thickness remained unchanged in both eyes during follow up in both patients.

Conclusion: This is the first report to describe the relationship between subfoveal choroidal thickness and MEWDS. We found that the choroid was thicker in the acute phase than the convalescent phase in both the affected and opposite eyes of both patients, suggesting that an inflammatory reaction might occur in the choroidal stroma in addition to the choriocapillaris and might be bilateral rather than unilateral.

Key words: choroidal inflammatory disease, choroidal thickness, optical coherence tomography, statins, white dot syndrome

Multiple evanescent white dot syndrome (MEWDS), first described in 1984 by Jampol and colleagues[1] and Sieving and colleagues,[2] is a typically unilateral retinopathy with sudden onset of vision loss that occurs predominantly in young females. Ophthalmoscopic examination in patients with MEWDS reveals multiple faint, yellow-white spots in the posterior pole to the midperipheral fundus. The disease is self-limiting with almost all patients regaining good visual acuity

within several weeks. Fluorescein angiography (FA) shows hyperfluorescence of the yellow-white spots, whereas late-phase indocyanine green angiography (ICGA) reveals more hypofluorescent spots than what is seen with fluorescein angiography.[3,4] Although the pathogenesis of MEWDS remains unknown, electroretinography and electrooculography have revealed dysfunction of the photoreceptors and retinal pigment epithelium.[5–7]

Recent spectral-domain optical coherence tomographic (SD-OCT) studies have noted disruptions in the photoreceptor inner segment/outer segment junction (IS/OS) in patients with acute phase MEWDS, but no pathological changes in the retinal pigment epithelium or choroid.[8,9] Here, we investigate changes in subfoveal choroidal thickness between acute and convalescent phases in two patients with MEWDS.

METHODS

This study was conducted under a retrospective design in two patients diagnosed with MEWDS. They had undergone a comprehensive ophthalmic examination, including assessment of visual acuity (VA), slitlamp biomicroscopy, dilated funduscopy and fluorescein angiography (VISUCAM NM/FA; Carl Zeiss Meditec AG, Dublin, CA, USA). We also performed indocyanine green angiography using a scanning laser ophthalmoscope Model 101 (Rodenstock Instruments, Munich, Germany) in one of the two patients.

Cross-sectional retinal images were evaluated using SD-OCT (Cirrus HD-OCT, Carl Zeiss Meditec AG) in both patients. The SD-OCT was taken horizontally through the centre of the fovea (6.0 mm line) using programs with either five-line raster or HD five-line raster. Using the Cirrus linear measurement tool, two independent observers manually measured subfoveal choroidal thickness from the posterior edge of the retinal pigment epithelium to the choroid/sclera junction at the position of the foveal depression, in accordance with a previously published method.[10] The average of the obtained measurements was determined as the subfoveal choroidal thickness. Similarly, the central retinal thickness (at the position of the foveal depression) was manually measured at this time to compare changes in both retinal and choroidal thickness during follow-up periods.

RESULTS

Patient 1

A 21-year-old female Japanese patient with no previous history of ocular disease presented to our hospital with sudden loss of visual acuity in the right eye. On initial examination, VA was 0.2 (with -11.00 DS) in the right eye and 1.2 (with -9.00 DS) in the left eye. No inflammatory cells were observed in the anterior segment or vitreous of either eye. Fundus examination revealed foveal granularity and scattered yellow-white spots in the posterior pole in the right eye (Figure 1A). Early phase fluorescein angiography in the right eye showed small hyperfluorescent lesions that were determined to be retinal spots (Figure 1B). Late-phase ICGA of the right eye revealed numerous hypofluorescent spots throughout the posterior pole (Figure 1C). In contrast, no significant findings were noted in the left eye on funduscopy, fluorescein angiography or indocyanine green angiography. SD-OCT of the right eye revealed a disrupted external limiting membrane (ELM) and IS/OS lines in the foveal region (Figure 2A). There was no evidence of systemic inflammation (normal erythrocyte sedimentation rate and C-reactive protein levels). No therapy was administered.

Five weeks after the initial visit, VA had recovered to 1.0, all evidence of foveal granularity and yellow-white spots had disappeared (Figure 1D) and the ELM and IS/OS lines had been restored without therapy. At the final visit (345 days after the initial visit), VA was 1.2 and ELM and IS/OS lines in the right eye were preserved (Figure 2C).

Patient 2

A 16-year-old female Japanese patient with a history of familial hypercholesterolaemia and simvastatin treatment was referred to our hospital three days after complaining of blurred vision in the right eye. She reported flu-like symptoms seven days before the initial visit. On initial examination, VA was 1.2 (-3.00 DS) in the right eye and 0.8 (-3.00 DS) in the left eye. No significant findings were observed in the anterior segment or vitreous of either eye. Funduscopy revealed foveal granularity and faint, scattered, yellow-white spots in the posterior pole in the left eye (Figure 1E). While early phase fluorescein angiography in the left eye showed small hyperfluorescent retinal spots (Figure 1F), the right eye appeared normal on funduscopy or fluorescein angiography. SD-OCT in the left eye revealed a disrupted IS/OS line in the foveal region (Figure 2B). There was no evidence of systemic inflammation and no therapy was administered.

Subjective visual improvement was reported within several days from the onset of the symptom. VA recovered to 1.2 six days after the initial visit, and after one month the foveal granularity and yellow-white spots had disappeared entirely (Figure 1G) and the IS/OS line was restored. At the final visit (133 days after the initial visit), VA was 1.5 and the IS/OS line in the left eye was found to be preserved (Figure 2D). The simvastatin treatment has been continued during the follow-up period.

Assessment of subfoveal choroidal and central retinal thickness

In Patient 1, while the subfoveal choroidal thickness at the initial visit (acute phase) was 337 µm in the affected right eye (Figures 2A and 3A), this thickness markedly decreased to 249 µm at 133 days after the initial visit (convalescent phase) and measured 243 µm on the final visit (345 days after the initial visit) (Figure 3A). The subfoveal choroidal thickness in the opposite left eye also decreased over the course of follow up, from 277 µm to 241 µm (Figure 3A).

Similarly, in Patient 2, the subfoveal choroidal thickness at the initial visit (acute phase) was 440 µm in the affected left eye (Figures 2B and 3B) but markedly

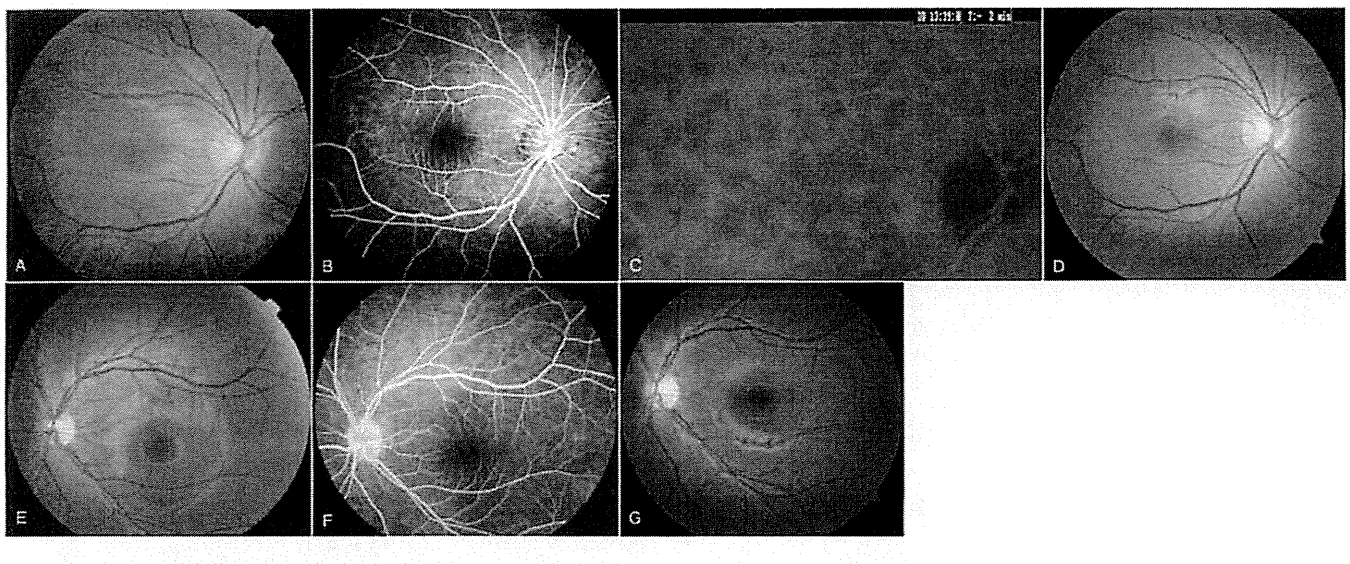

Figure 1. Fundus images of the right eye of Patient 1 (A–D) and the left eye of Patient 2 (E–G).
Fundus photograph showing foveal granularity and scattered yellow-white spots in the posterior pole (A). Early phase fluorescein angiographic image showing small hyperfluorescent retinal spots (B). Late-phase indocyanine green angiographic image showing numerous hypofluorescent spots throughout the posterior pole (C). Fundus photograph showing that the foveal granularity and yellow-white spots had disappeared at five weeks after the initial visit (D). Fundus photograph showing foveal granularity and faint, scattered, yellow-white spots in the posterior pole (E). Early phase fluorescein angiographic image showing small hyperfluorescent retinal spots (F). Fundus photograph showing that the foveal granularity and yellow-white spots had disappeared one month after the initial visit (G).

decreased to 358 μm at the final visit (133 days after the initial visit, convalescent phase) (Figures 2D and 3B). The subfoveal choroidal thickness in the opposite eye (RE) also decreased, from 382 μm to 331 μm (Figure 3B).

In both patients, the choroidal stromal vessels in the acute phase (Figures 2A and 2B) were more dilated than in the convalescent phase (Figures 2C and 2D); however, no change was noted in the central retinal thickness of either eye of either patient (Figures 3C and 3D for Patients 1 and 2, respectively) during the follow-up periods.

DISCUSSION

Here, we report new SD-OCT findings in two patients with MEWDS. The subfoveal choroidal thickness in patients during the acute phase was considerably thicker than in the convalescent phase, not only in the affected eye but also in the asymptomatic opposite eye. In addition, thickness during the acute phase was thicker in the affected eye than in the opposite eye in both patients.

Although the aetiology of MEWDS is not well understood, fluorescein angiographic and electrophysiological studies have suggested that this inflammatory disease affects the retinal pigment epithelium and outer retina. Subsequently, several reports have suggested that the numerous hypofluorescent spots noted on ICGA are likely to be due to hypoperfusion of the choriocapillaris, making the disease primary inflammation of the choriocapillaris.[11,12] Schaal and colleagues[13] reported a single case of simultaneous appearance of MEWDS and multifocal choroiditis, suggesting a possible common causal entity.

In contrast to indocyanine green angiographic findings, recent SD-OCT studies have noted no abnormalities in the retinal pigment epithelial layer or choroid in MEWDS patients,[8,9] although choroidal thickness has not been compared between the acute and convalescent phases. SD-OCT findings for affected eyes in the present study revealed a marked decrease in subfoveal choroidal thickness from the acute phase without therapy in both patients after four or more months (Figures 2 and 3). A recent study described electroretinographic and SD-OCT findings in seven patients with MEWDS,[7] noting that the choroidal thickness and the choroidal stromal vessels in the convalescent phase (four months after the initial visit) appeared to be reduced over values in the acute phase in at least one (Patient 1 in Figure 2[7]) of the seven patients, although the authors did not explicitly mention choroidal thickness.[7] The SD-OCT findings in our two patients showed greater dilation in the choroidal stromal vessels during the acute phase (Figures 2A and 2B) compared with the convalescent phase (Figures 2C and 2D),

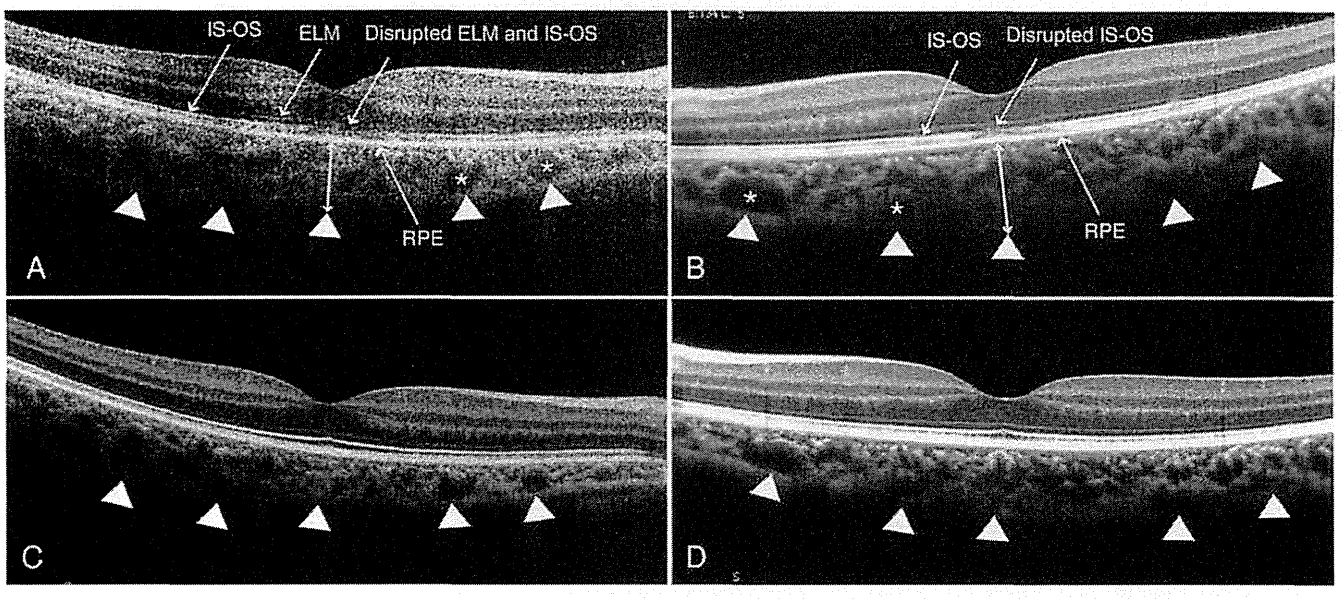

Figure 2. Horizontal scan images (6.0 mm) of spectral-domain optical coherence tomography (SD-OCT) of the right eye of Patient 1 (A and C) and the left eye of Patient 2 (B and D).
The SD-OCT images reveal a disrupted external limiting membrane (ELM) and photoreceptor inner segment/outer segment junction (IS/OS) lines in the foveal region (A) and a disrupted IS/OS line in the foveal region (B) in the acute phase. The asterisks indicate dilated choroidal stromal vessels (A and B). The SD-OCT images show restoration of the ELM line and IS/OS lines at the final visit (345 days after the initial visit) (C) and restoration of the IS/OS line at the final visit (133 days after the initial visit) (D) in the convalescent phase. The arrowheads indicate the choroid/sclera junction (A–D). The double-headed arrows indicate subfoveal choroidal thickness (A and B). The subfoveal choroidal thickness markedly decreased from 337 μm (A) to 249 μm (C) in Patient 1 and from 440 μm (B) to 358 μm (D) in Patient 2.

suggesting that choroidal thickening might be due to dilation of the choroidal stromal vessels. These present and previous findings suggest that in addition to a disrupted IS/OS line, choroidal thickening might be a feature of the acute phase of MEWDS (Figures 2A and 2B).[7–9]

Marked increases in choroidal thickness can be observed in patients with Vogt–Koyanagi–Harada (VKH) disease[14] or central serous chorioretinopathy (CSC).[15,16] VKH disease is a bilateral granulomatous uveitis, in which the target of the inflammatory reaction is located within the choroidal stroma, making the disease primary stromal choroiditis.[17] While the increased choroidal thickness in VKH disease might be related to inflammatory infiltration or increased exudation,[14] the thickening in central serous chorioretinopathy, which is characterised by an idiopathic and mostly unilateral serous retinal detachment in the posterior pole,[18] has been confirmed to be due to choroidal vascular hyperpermeability.[15,16] While typically seen in patients with VKH or CSC, no leakage or hyperpermeability of choroidal stromal vessels is noted with indocyanine green angiography in the acute phase of MEWDS;[12,19] however, several studies[1,20] of MEWDS patients have reported focal segmental staining of choroidal vessels and discrete nodular hyperfluorescent areas in the inner choroid with ICGA. Taken together, these findings suggest that an inflammatory reaction might also occur at the level of the choroidal stroma in addition to the choriocapillaris.

In most patients with MEWDS, recovery of visual function occurs within several weeks.[19] Interestingly, Patient 2, who had simvastatin treatment, reported a more rapid improvement in both symptoms and visual acuity. Simvastatin belongs to the class of cholesterol-lowering statins. It has been proposed that statins have anti-inflammatory effects that are not directly related to their cholesterol-lowering activity.[21,22] Although anti-inflammatory effects of statins have not been demonstrated in inflammatory choroidal disease, the rapid visual improvement in Patient 2 might be associated with simvastatin treatment.

Explaining why choroidal thickening was observed even in the asymptomatic opposite eyes in the present study is difficult (Figures 3A and 3B). A recent study[7] observed that five of seven patients with unilateral MEWDS manifested visual field abnormalities in both eyes, not just the affected eyes, during the acute phase, suggesting that visual dysfunction is bilateral

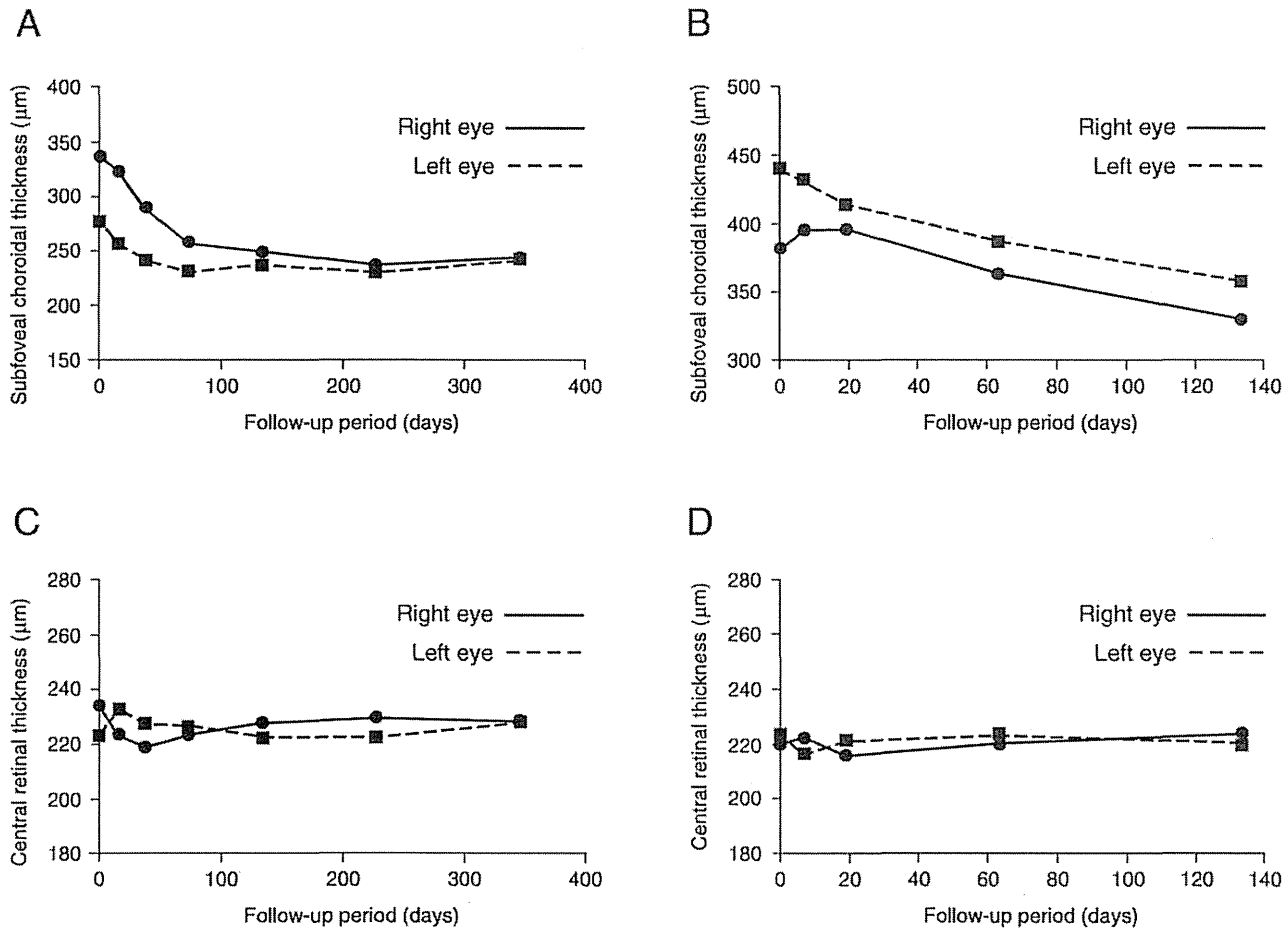

Figure 3. Changes in subfoveal choroidal thickness (A and B) and central retinal thickness (C and D) during the follow-up period for Patients 1 (A and C) and 2 (B and D).
In Patient 1, the subfoveal choroidal thickness at the initial visit (day zero, acute phase) in the right eye was 337 μm (A), markedly decreased to 249 μm (day 133, convalescent phase) and was 243 μm at the final visit (Day 345) (A). The thickness in the left eye (asymptomatic opposite eye) also decreased from 277 μm (day zero) to 241 μm (day 345) (A). Similarly, in Patient 2, the subfoveal choroidal thickness at the initial visit (day zero, acute phase) in the left eye was 440 μm (B) and markedly decreased to 358 μm at the final visit (day 133, convalescent phase) (B). The thickness in the right eye (asymptomatic opposite eye) also decreased from 382 μm (day zero) to 331 μm (day 133) (B). No changes were noted in central retinal thickness for either eye of Patients 1 (C) or 2 (D) during the follow-up period.

in most patients. Given these present and previous findings, the inflammatory reaction in MEWDS might occur bilaterally more often than unilaterally, even though the condition is believed to be unilateral in most patients.

In conclusion, this is the first report to describe the relationship between subfoveal choroidal thickness and MEWDS. We noted the previously unreported finding that choroid thickness was greater in the acute phase than in the convalescent phase in both eyes, not just the affected eyes, suggesting that an inflammatory reaction might occur in the choroidal stroma in addition to the choriocapillaris. Because our findings were derived from only two patients, further study is needed to determine the presence of choroidal thickening in other patients with MEWDS.

GRANTS AND FINANCIAL SUPPORT
This study was supported by grants from the Ministry of Education, Culture, Sports, Science and Technology of Japan (Grant-in-Aid for Scientific Research) (TH), The Jikei University Research Fund (TH) and

the Vehicle Racing Commemorative Foundation (TH and HT).

REFERENCES

1. Jampol LM, Sieving PA, Pugh D, Fishman GA, Gilbert H. Multiple evanescent white dot syndrome. I. Clinical findings. *Arch Ophthalmol* 1984; 102: 671–674.
2. Sieving PA, Fishman GA, Jampol LM, Pugh D. Multiple evanescent white dot syndrome. II. Electrophysiology of the photoreceptors during retinal pigment epithelial disease. *Arch Ophthalmol* 1984; 102: 675–679.
3. Ie D, Glaser BM, Murphy RP, Gordon LW, Sjaarda RN, Thompson JT. Indocyanine green angiography in multiple evanescent white-dot syndrome. *Am J Ophthalmol* 1994; 117: 7–12.
4. Gross NE, Yannuzzi LA, Freund KB, Spaide RF, Amato GP, Sigal R. Multiple evanescent white dot syndrome. *Arch Ophthalmol* 2006; 124: 493–500.
5. Laatikainen L, Immonen I. Multiple evanescent white dot syndrome. *Graefes Arch Clin Exp Ophthalmol* 1988; 226: 37–40.
6. Feigl B, Haas A, El-Shabrawi Y. Multifocal ERG in multiple evanescent white dot syndrome. *Graefes Arch Clin Exp Ophthalmol* 2002; 240: 615–621.
7. Li D, Kishi S. Restored photoreceptor outer segment damage in multiple evanescent white dot syndrome. *Ophthalmology* 2009; 116: 762–770.
8. Nguyen MH, Witkin AJ, Reichel E, Ko TH, Fujimoto JG, Schuman JS, Duker JS. Microstructural abnormalities in MEWDS demonstrated by ultrahigh resolution optical coherence tomography. *Retina* 2007; 27: 414–418.
9. Hangai M, Fujimoto M, Yoshimura N. Features and function of multiple evanescent white dot syndrome. *Arch Ophthalmol* 2009; 127: 1307–1313.
10. Manjunath V, Taha M, Fujimoto JG, Duker JS. Choroidal thickness in normal eyes measured using Cirrus HD optical coherence tomography. *Am J Ophthalmol* 2010; 150: 325–329.
11. Herbort CP. Inflammatory choriocapillaropathies: general concepts. In: Gupta A, Gupta G, Herbort CP, Khairallah M, eds. Uveitis Text and Imaging. New Delhi: Jaypee Brothers Medical Publishers, 2009. p 430–441.
12. Herbort CP. Multiple evanescent white dot syndrome (MEWDS) and acute idiopathic blind spot enlargement (AIBSE). In: Gupta A, Gupta G, Herbort CP, Khairallah M, eds. Uveitis Text and Imaging. New Delhi: Jaypee Brothers Medical Publishers, 2009. p 441–447.
13. Schaal S, Schiff WM, Kaplan HJ, Tezel TH. Simultaneous appearance of multiple evanescent white dot syndrome and multifocal choroiditis indicate a common causal relationship. *Ocul Immunol Inflamm* 2009; 17: 325–327.
14. Maruko I, Iida T, Sugano Y, Oyamada H, Sekiryu T, Fujiwara T, Spaide RF. Subfoveal choroidal thickness after treatment of Vogt–Koyanagi–Harada disease. *Retina* 2011; 31: 510–517.
15. Imamura Y, Fujiwara T, Margolis R, Spaide RF. Enhanced depth imaging optical coherence tomography of the choroid in central serous chorioretinopathy. *Retina* 2009; 29: 1469–1473.
16. Maruko I, Iida T, Sugano Y, Ojima A, Ogasawara M, Spaide RF. Subfoveal choroidal thickness after treatment of central serous chorioretinopathy. *Ophthalmology* 2010; 117: 1792–1799.
17. Bouchenaki N, Herbort CP. Stromal choroiditis. In: Pleyer U, Mondino B, eds. Uveitis and Immunological Disorders. Berlin: Springer, 2004. p 233–253.
18. Klais CM, Ober MD, Ciardella AP, Yannuzzi LA. Central serous chorioretinopathy. In: Ryan SJ, ed. Retina. 4th ed. Vol 2. Philadelphia: Elsevier Mosby, 2006. p 1135–1161.
19. Tsai LM, Jampol LM. Multiple evanescent white-dot syndrome. In: Ryan SJ, ed. Retina. 4th ed. Vol 2. Philadelphia: Elsevier Mosby, 2006. p 1785–1791.
20. Sikorski BL, Wojtkowski M, Kaluzny JJ, Szkulmowski M, Kowalczyk A. Correlation of spectral optical coherence tomography with fluorescein and indocyanine green angiography in multiple evanescent white dot syndrome. *Br J Ophthalmol* 2008; 92: 1552–1557.
21. Diomede L, Albani D, Sottocorno M, Donati MB, Bianchi M, Fruscella P, Salmona M. In vivo anti-inflammatory effect of statins is mediated by non-sterol mevalonate products. *Arterioscler Thromb Vasc Biol* 2001; 21: 1327–1332.
22. Bartoli M, Al-Shabrawey M, Labazi M, Behzadian MA, Istanboli M, El-Remessy AB, Cardwell AW et al. HMG-CoA reductase inhibitors (statin) prevents retinal neovascularization in a model of oxygen-induced retinopathy. *Invest Ophthalmol Vis Sci* 2009; 50: 4934–4940.

Corresponding author:
Dr Takaaki Hayashi
Department of Ophthalmology
The Jikei University School of Medicine
3-25-8 Nishi-shimbashi Minato-ku
Tokyo, 105-8461
JAPAN
E-mail: taka@jikei.ac.jp